PHYSICAL REVIEW C **93**, 025201 (2016)

Role of pentaquark components in ϕ meson production proton-antiproton annihilation reactions

S. Srisuphaphon,[1,2] A. Kaewsnod,[3] A. Limphirat,[2,3] K. Khosonthongkee,[2,3] and Y. Yan[2,3,*]
[1]*Department of Physics, Faculty of Science, Burapha University, Chonburi 20131, Thailand*
[2]*Thailand Center of Excellence in Physics, Ministry of Education, Bangkok, Thailand*
[3]*School of Physics, Institute of Science, Suranaree University of Technology, Nakhon Ratchasima 30000, Thailand*
(Received 29 July 2015; published 3 February 2016)

The pentaquark component $uuds\bar{s}$ is included in the proton wave functions to study ϕ meson production proton-antiproton annihilation reactions. With all possible configurations of the *uuds* subsystem proposed for describing the strangeness spin and magnetic moment of the proton, we estimate the branching ratios of the annihilation reactions at rest $p\bar{p} \to \phi X$ ($X = \pi^0, \eta, \rho^0, \omega$) from atomic $p\bar{p}$ *S*- and *P*-wave states by using effective quark line diagrams incorporating the $^3P_0$ model. The best agreement of theoretical prediction with the experimental data is found when the pentaquark configuration of the proton wave function takes the flavor-spin symmetry $[4]_{\rm FS}[22]_F[22]_S$.

DOI: 10.1103/PhysRevC.93.025201

I. INTRODUCTION

The apparent Okubo-Zweig-Iizuka (OZI) rule violation in ϕ production nucleon-antinucleon annihilation reactions suggests the existence of strange quarks in the nucleon [1,2]. There are also other experimental results indicating the strangeness content in the nucleon; for example, the strange quark-antiquark contributions to the electric and magnetic strange form factors of the nucleon in parity violation experiments of electron scattering from the nucleon [3]. The strangeness magnetic moment μ_s is obtained by extrapolating the magnetic strange form factors $G_M^s(Q^2)$ at momentum transfer $Q^2 = 0$, which suggests a positive value for μ_s [4], but most theoretical calculations in the $3q$ picture of the proton derive a negative value for this observable, as reviewed in Refs. [5,6].

There is an interesting work in which the strangeness magnetic moment of the proton is studied by including the pentaquark component $uuds\bar{s}$, in addition to the $3q$ component (*uud*), into the proton wave function [7]. It is shown in Ref. [7] that almost all $5q$ configurations give the strangeness spin contribution σ_s a negative value, consistent with the experimental and theoretical indications of the spin structure of the proton [8]. However, only the $5q$ configurations, where the subsystem *uuds* is in the *S* state but the $\bar{s}$ is in the *P* state relative to the *uuds* subsystem, result in negative values for μ_s, while positive values for μ_s are found in the $5q$ configurations where the subsystem *uuds* is in the *P* state but the $\bar{s}$ is in the *S* state relative to the *uuds* subsystem. The proposed pentaquark picture has been applied to other works such as the estimation of the admixture $uuds\bar{s}$ component in the nucleon wave function with the strangeness form factor of the proton [9–11], the study of the amplitudes for the electromagnetic transition $\gamma^* N \to N^*(1535)$ [12], and the electromagnetic decay of the $N(1440)$ resonance [13,14].

The recent report by the LHCb Collaboration [15] of two charmonium pentaquark states $P_c^+(4380)$ and $P_c^+(4450)$ has cast more light on the works in which the pentaquark configuration is considered a possible component of the nucleon.

In the present work we study ϕ meson production proton-antiproton annihilation reactions $p\bar{p} \to \phi X$ ($X = \pi^0,\eta,\rho^0,\omega$), considering all possible $uuds\bar{s}$ configurations for the proton wave function in addition to the $3q$ component. In our previous work [16], the proton-antiproton annihilation reactions have been studied with the $5q$ components in three models, namely, the *uud* cluster with a $s\bar{s}$ sea quark component, kaon-hyperon clusters based on the chiral quark model, and the pentaquark picture $uuds\bar{s}$ where the subsystem *uuds* is in the *S* state but the $\bar{s}$ is in the *P* state relative to the *uuds* subsystem, resulting in negative values for the σ_s. In the case of the pentaquark picture, two configurations of $uuds\bar{s}$, the mixed flavor-spin symmetries $[31]_{\rm FS}[211]_F[22]_S$ and $[31]_{\rm FS}[31]_F[22]_S$, were considered, since these two configurations result in negative values for σ_s and μ_s. For the atomic $p\bar{p}$ *S*-wave states, the theoretical branching ratios in comparison with experimental data were discussed and listed in Table III in Ref. [16].

There are 15 possible $5q$ configurations, where the subsystem *uuds* is in the *P* state but the $\bar{s}$ is in the *S* state relative to the *uuds* subsystem, resulting in negative values for the σ_s. It is shown in Ref. [7] that the configuration with $[4]_{\rm FS}[22]_F[22]_S$ flavor-spin symmetry is likely to have the lowest energy. In this work, we study the proton-antiproton annihilation reactions from atomic $p\bar{p}$ *S*- and *P*-wave states, focusing on these 15 configurations. The paper is organized as follows. Proton wave functions with various $5q$ component are constructed in Section II. In Sec. III we evaluate the branching ratios for the reactions $p\bar{p} \to \phi X$. Finally a summary and conclusions are given in Sec. IV.

II. PROTON WAVE FUNCTIONS WITH PENTAQUARK COMPONENTS

According to the OZI rule, violations in the $N\bar{N}$ annihilation reactions involving the ϕ meson suggest the presence of an intrinsic $s\bar{s}$ in the nucleon wave function. The proton wave

*Corresponding author: yupeng@sut.ac.th

function with the addition of $uuds\bar{s}$ components to the uud quark component have been written generally in the form [17]

$$|p\rangle = A|uud\rangle + B|uuds\bar{s}\rangle, \tag{1}$$

where A and B are the amplitude factors for the uud and $uuds\bar{s}$ components in the proton, respectively. It is suggested that the strange quark contribution to the strangeness σ term appears to lie somewhere in the range of 2–7% of the nucleon mass [18]. Therefore, the strangeness admixture can be treated as a small perturbation in the proton wave function, that is, $B^2 \ll A^2$. However, the five-quark component is the main contribution to the ϕ production in $p\bar{p}$ annihilation. The $5q$ states may be constructed by coupling the $uuds$ wave function with the $\bar{s}$ one.

In the language of group theory, the permutation symmetry of the four-quark configuration is characterized by the S_4 Young tabloids [4], [31], [22], [211], and [1111]. That the pentaquark wave function should be a color singlet demands that the color part of the pentaquark wave function must be a $[222]_1$ singlet. The color state of the antiquark in pentaquarks is a [11] antitriplet, thus the color wave function of the four-quark configuration must be a $[211]_3$ triplet,

$$\chi^c_{[211]_\lambda}(q^4) = \begin{array}{|c|c|}\hline 1 & 2 \\ \hline 3 & \\ \cline{1-1} 4 & \\ \cline{1-1}\end{array}\,, \quad \chi^c_{[211]_\rho}(q^4) = \begin{array}{|c|c|}\hline 1 & 3 \\ \hline 2 & \\ \cline{1-1} 4 & \\ \cline{1-1}\end{array}\,,$$
$$\chi^c_{[211]_\eta}(q^4) = \begin{array}{|c|c|}\hline 1 & 4 \\ \hline 2 & \\ \cline{1-1} 3 & \\ \cline{1-1}\end{array}\,. \tag{2}$$

The q^4 color wave functions can be derived by applying the λ-type, ρ-type, and η-type projection operators of the irreducible representation IR[211] of the permutation group S_4 in Yamanouchi basis onto single-particle color states. The details can be found in Ref. [19] and Appendix A. The singlet color wave function of the pentaquark at color symmetry pattern $j = \lambda,\rho,\eta$ is given by

$$\chi^C_{[222]_j} = \frac{1}{\sqrt{3}}\left[\chi^c_{[211]_j}(R)\,\bar{R} + \chi^c_{[211]_j}(G)\,\bar{G} + \chi^c_{[211]_j}(B)\,\bar{B}\right]. \tag{3}$$

The total wave function of the four quark configuration is antisymmetric, implying that the spatial-spin-flavor part must be a [31] state. The total wave function of the q^4 configuration may be written in the general form

$$\psi_{[1111]} = \sum_{i,j=\lambda,\rho,\eta} a_{ij}\,\chi^c_{[211]_i}\chi^{\text{osf}}_{[31]_j}. \tag{4}$$

The coefficients a_{ij} can be determined easily by applying the IR[31] and IR[211] of the permutation group S_4 in Yamanouchi basis onto the equation. The total wave function of the q^4 subsystem takes the form

$$\psi_{[1111]} = \frac{1}{\sqrt{3}}\left(\chi^c_{[211]_\lambda}\chi^{\text{osf}}_{[31]_\rho} - \chi^c_{[211]_\rho}\chi^{\text{osf}}_{[31]_\lambda} + \chi^c_{[211]_\eta}\chi^{\text{osf}}_{[31]_\eta}\right). \tag{5}$$

TABLE I. Spatial-spin-flavor configurations of q^4 clusters.

$[31]_{\text{OSF}}$	
$[4]_O$	$[31]_{\text{SF}}$
$[1111]_O$	$[211]_{\text{SF}}$
$[22]_O$	$[31]_{\text{SF}},[211]_{\text{SF}}$
$[211]_O$	$[31]_{\text{SF}},[211]_{\text{SF}},[22]_{\text{SF}}$
$[31]_O$	$[4]_{\text{SF}},[31]_{\text{SF}},[211]_{\text{SF}},[22]_{\text{SF}}$

The spatial-spin-flavor and spin-flavor states of the q^4 cluster in the above equation can be written in the general forms

$$\chi^{\text{osf}}_{[31]} = \sum_{i,j} a_{ij}\,\chi^o_{[X]_i}\chi^{sf}_{[Y]_j}, \tag{6}$$

$$\chi^{sf}_{[Z]} = \sum_{i,j} a_{ij}\,\chi^f_{[X]_i}\chi^s_{[Y]_j}, \tag{7}$$

where χ^o_i, χ^f_i, and χ^s_i are respectively the q^4 spatial, flavor, and spin wave functions of symmetry (S), antisymmetry (A), λ type, ρ type, and η type. The possible spatial-spin-flavor and spin-flavor configurations and explicit forms of the wave functions are determined by applying the S_4 representations in Yamanouchi basis. Listed in Tables I and II are respectively the possible spatial-spin-flavor and spin-flavor configurations.

According to the requirement of positive parity for the proton wave function, if the $uuds$ subsystem is in the ground state then the relative angular momentum between the subsystem and the $\bar{s}$ must be odd. For the $uuds$ subsystem in the ground state, the spatial part of the subsystem takes the $[4]_O$ symmetry and hence the spin-flavor part must take the $[31]_{\text{FS}}$ symmetry as shown in Table I in order to form an antisymmetric spatial-color-spin-flavor $uuds$ part of the pentaquark wave function. If the spin symmetry of the $uuds$ subsystem is described by $[22]_S$ corresponding to spin 0, the flavor symmetry representations $[31]_F$ and $[211]_F$ may combine with the spin symmetry state $[22]_S$ to form the mixed symmetry spin-flavor states $[31]_{\text{FS}}$ as shown in Table II here and in Ref. [7]. In this case, the $5q$ component may be written

TABLE II. Spin-flavor configurations of q^4 clusters.

	$[4]_{\text{FS}}$		
$[22]_F[22]_S$	$[31]_F[31]_S$	$[4]_F[4]_S$	
	$[31]_{\text{FS}}$		
$[31]_F[22]_S$	$[31]_F[31]_S$	$[31]_F[4]_S$	$[211]_F[22]_S$
$[211]_F[31]_S$	$[22]_F[31]_S$	$[4]_F[31]_S$	
	$[22]_{\text{FS}}$		
$[22]_F[22]_S$	$[22]_F[4]_S$	$[4]_F[22]_S$	$[211]_F[31]_S$
$[31]_F[31]_S$			
	$[211]_{\text{FS}}$		
$[211]_F[22]_S$	$[211]_F[31]_S$	$[211]_F[4]_S$	$[22]_F[31]_S$
$[31]_F[22]_S$	$[31]_F[31]_S$		

in the general form

$$|uuds\bar{s}\rangle = \left[\left|\frac{1}{2},m_{\bar{s}}\right\rangle \otimes |1,\mu\rangle\right]_{\frac{1}{2},m_{5q}} \frac{1}{\sqrt{3}}\big(\chi^{C}_{[222]_\lambda}\big(\bar{s}\chi^{FS}_{[31]_\rho}\big) - \chi^{C}_{[222]_\rho}\big(\bar{s}\chi^{FS}_{[31]_\lambda}\big) + \chi^{C}_{[222]_\eta}\big(\bar{s}\chi^{FS}_{[31]_\eta}\big)\big), \quad (8)$$

where $(\frac{1}{2},m_{5q})$ denotes the spin of the $5q$ component. The spin state of $\bar{s}$ and the angular momentum $\ell = 1$ are denoted by $|\frac{1}{2},m_{\bar{s}}\rangle$ and $|1,\mu\rangle$, respectively. The function $\chi^{FS}_{[31]_{(\lambda,\rho,\eta)}}$ represents the coupled spin-flavor part with the mixed symmetry $[31]_{FS}$. The $5q$ component with the configurations $[31]_{FS}[211]_F[22]_S$ and $[31]_{FS}[31]_F[22]_S$ results in negative values for σ_s and μ_s [7].

For the P-state $uuds$ subsystem, in the language of group theory, the orbital angular momentum $\ell = 1$ means that the spatial wave function of the subsystem has the mixed symmetry $[31]_O$. Therefore, the possible spin-flavor configurations are $[4]_{FS}$, $[31]_{FS}$, $[211]_{FS}$, and $[22]_{FS}$, as shown in Table II, which couple with the $[31]_O$ spatial state to form the $[31]_{OSF}$ spatial-flavor-spin components of the $uuds$ subsystem. There are three possible spin symmetries of the $uuds$ subsystem: $[22]_S$, $[31]_S$, and $[4]_S$ representations as shown in Table I, corresponding to spin $S = 0, 1, 2$, respectively. For this case, the full wave functions of the $5q$ component will be presented in Sec. III.

III. THE $N\bar{N}$ TRANSITION AMPLITUDE AND BRANCHING RATIOS

In this work we study the annihilation reactions $N\bar{N} \to X\phi(X = \pi^0,\eta,\rho^0,\omega)$ with the effective quark line diagram for the shake-out of a ϕ meson from the $5q$ component, as described in Fig. 1 [17].

According to the quark diagram, the transition amplitudes from the $5q$ component $|uuds\bar{s}\rangle$ and the antiproton $|\bar{u}\bar{u}\bar{d}\rangle$ wave function in the momentum space representation are given by

$$T_{A_1} = 2AB \int d^3q_1 \cdots d^3q_8 d^3q_{1'} \cdots d^3q_{4'} \langle \phi X|\vec{q}_{1'} \cdots \vec{q}_{4'}\rangle \times \langle \vec{q}_{1'} \cdots \vec{q}_{4'}|\mathcal{O}_{A_1}|\vec{q}_1 \cdots \vec{q}_8\rangle \langle \vec{q}_1 \cdots \vec{q}_8|(uuds\bar{s}) \otimes (\bar{u}\bar{u}\bar{d})\rangle. \quad (9)$$

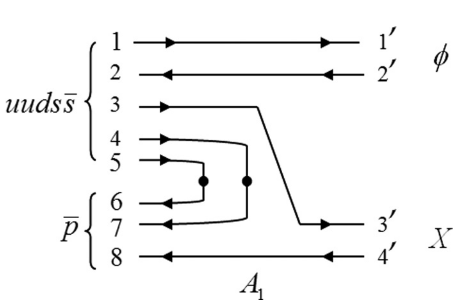

FIG. 1. The quark line diagram corresponding to the production of two meson final states in $p\bar{p}$ annihilation [17,20]. The dots refer to the effective vertex of the $^3P_0$ for $q\bar{q}$ pairs destroyed with the quantum numbers of the vacuum: $^3P_0$, isospin $I = 0$, and color singlet [21].

The effective operators $\mathcal{O}_{A_I}$, corresponding to the quark line diagram, take the form

$$\mathcal{O}_{A_1} = \lambda_{A_1}\delta^{(3)}(\vec{q}_1 - \vec{q}_{1'})\delta^{(3)}(\vec{q}_2 - \vec{q}_{2'})\delta^{(3)}(\vec{q}_3 - \vec{q}_{3'})\delta^{(3)} \times (\vec{q}_8 - \vec{q}_{4'})V^{56}V^{47}, \quad (10)$$

where λ_{A_1} is a parameter describing the effective strength of the transition topology which can be fitted by experimental data. The $^3P_0$ quark-antiquark vertex is defined as

$$V^{ij} = \sum_{\mu} \sigma^{ij}_{-\mu} Y_{1\mu}(\vec{q}_i - \vec{q}_j)\delta^{(3)}(\vec{q}_i + \vec{q}_j)(-1)^{1+\mu} 1^{ij}_F 1^{ij}_C, \quad (11)$$

where $\sigma^{ij}_{-\mu}$ is the spin operator for destroying $q_i\bar{q}_j$ pairs with spin 1 while $Y_{1\mu}(\vec{q})$ is the spherical harmonics in momentum space [22]. The unit operators in flavor and color spaces are denoted by 1^{ij}_F and 1^{ij}_C, respectively. Nevertheless, if the $5q$ component is treated as a small perturbative admixture in the proton ($B^2 \ll 1$), the transition amplitude with the term $\langle \vec{q}_1 \cdots \vec{q}_8|(uuds\bar{s}) \otimes (\bar{u}\bar{u}\bar{d}\bar{s}s)\rangle$ corresponding to the rearrangement process [17] can be ignored. The wave functions of the mesons M (ϕ and X) and $\bar{p}$ ($\bar{q}^3$) and $q^4\bar{q}$ states are given in Appendix B.

In the present work we consider the ϕ meson production $p\bar{p}$ annihilation reactions with the $5q$ component for the case of the subsystem $uuds$ in the P state. Fifteen possible configurations of $uuds\bar{s}$ will be considered. In order to involve relative motion, we choose the plane wave basis for the relative motions of $p\bar{p}$ and ϕX in the center-of-momentum system: $\delta^{(3)}(\vec{q}_1 + \vec{q}_2 + \vec{q}_3 + \vec{q}_4 + \vec{q}_5 - \vec{k})\delta^{(3)}(\vec{k} + \vec{q}_6 + \vec{q}_7 + \vec{q}_8)$ and $\delta^{(3)}(\vec{q} - \vec{q}_{1'} - \vec{q}_{2'})\delta^{(3)}(\vec{q} + \vec{q}_{3'} + \vec{q}_{4'})$, respectively. In the low-momentum approximation, as done in Ref. [16], the leading order of the transition amplitude $T^{SP(PS)}_{fi}$ for the S to P ($L = 0$, $\ell_f = 1$) and P to S ($L = 1$, $\ell_f = 0$) transitions from the initial state $|i\rangle$ to final state $|f\rangle$ with the quark line diagram A_1 can be obtained as

$$T^{SP(PS)}_{fi}(\vec{q},\vec{k}) = 2AB\lambda_{A_1} N\pi^4 q^{l_f} k^L \exp\{-Q^2_q q^2 - Q^2_k k^2\}\langle f|O_{A_1}|i\rangle, \quad (12)$$

where $N = N_\phi N_X N_{uuds\bar{s}} N_{\bar{p}}$ and

$$\langle f|O_{A_1}|i\rangle = \langle f| \sum_{\nu,\lambda}(-1)^{\nu+\lambda}\sigma^{56}_{-\nu}\sigma^{47}_{-\lambda} 1^{56}_F 1^{47}_F 1^{56}_C 1^{47}_C \times \sum_{m,n} \Omega^{SP(PS)}_{m,n} f^{SP(PS)}_{m,n}(\nu,\mu,\lambda,L,M,l_f,m_f)|i\rangle, \quad (13)$$

is the spin-color-flavor weight. Here Q^2_k, Q^2_q and $\Omega^{SP(PS)}_{m,n}$ are geometrical constants depending on the meson and baryon with $f^{SP(PS)}_{m,n}(\nu,\mu,\lambda,L,M,l_f,m_f)$ being the spin-angular momentum functions as shown in Appendix C.

In this work, we choose the radial parameter of the internal meson wave function $R_M = 4.1\ \text{GeV}^{-1}$, corresponding to the rms radius $\langle r^2\rangle^{1/2}_{S\text{-wave}} = 0.5$ fm of the $q\bar{q}$ system [22]. For the radial parameters of the proton, we use $R_B = 3.1\ \text{GeV}^{-1}$ for the q^3 wave function, leading to the rms radius $\langle r^2\rangle^{1/2} = 0.61$ fm for the q^3 component of the nucleon [23]. There is no solid evidence of the existence of a pentaquark state and, therefore, we have indeed no reliable knowledge of the length parameter of the q^5 wave function. The simplest way is to use the same length parameter for the q^5 wave function, that is, $R_{uuds\bar{s}} = 3.1\ \text{GeV}^{-1}$, which results in the rms radius $\langle r^2\rangle^{1/2} = 0.67$ fm for the q^5 component. Considering the small contribution of the q^5 component, the combined rms radius of the nucleon is almost the same as the rms radius of the q^3 component.

The initial state $|i\rangle$ and final state $|f\rangle$ can be written as

$$|i\rangle = \left|\left\{\chi_{\frac{1}{2},m_{5q}}(uuds\bar{s}) \otimes \chi_{\frac{1}{2},m_{\bar{p}}}(\bar{u}\bar{u}\bar{d})\right\}_{S,S_z} \otimes (L,M)\right\rangle_{J,J_z}, \quad (14)$$

$$|f\rangle = \left|\left\{\chi_{1,m_\alpha}(\phi) \otimes \chi_{j_m,m_{3',4'}}(X)\right\}_{j,m_\epsilon} \otimes (\ell_f,m_f)\right\rangle_{J,J_z}, \quad (15)$$

where $\chi_{\frac{1}{2},m_{5q}}(uuds\bar{s})$ is the spin-flavor-color part of the $5q$ component, L and l_f are respectively the initial and final orbital angular momenta, J is the total angular momentum, and I is the isospin. The matrix element $\langle f|O_{A_1}|i\rangle$ can be evaluated by using the two-body matrix elements for spin, flavor, and color, corresponding to the $^3P_0$ quark model,

$$\langle 0|\sigma_\upsilon^{ij}\left|\chi_{m_{ij}}^{J_{ij}}(ij)\right\rangle = \delta_{J_{ij},1}\delta_{m_{ij},-\upsilon}(-1)^\upsilon\sqrt{2}, \quad (16)$$

$$\langle 0|1_F^{ij}\left|\chi_{t_{ij}}^{T_{ij}}(ij)\right\rangle = \delta_{T_{ij},0}\delta_{t_{ij},0}\sqrt{2}, \quad (17)$$

and

$$\langle 0|1_C^{ij}\left|q_\alpha^i\bar{q}_\beta^j\right\rangle = \delta_{\alpha\beta}, \quad (18)$$

where α and β are the color indices.

Since we consider $p\bar{p}$ annihilations at rest, the proton-antiproton wave function is strongly correlated due to the $N\bar{N}$ interaction [24,25]. Therefore the initial state interaction for the atomic state of the $p\bar{p}$ system has to be involved [23], resulting in the transition amplitude

$$T_{f,i}(\vec{q}) = \int d^3k\, T_{fi}^{\text{SP(PS)}}(\vec{q},\vec{k})\phi_{\text{LSJ}}^I(\vec{k}), \quad (19)$$

where $\phi_{\text{LSJ}}^I(\vec{k})$ is the protonium wave function in the momentum space for fixed isospin I. With the transition amplitude, the partial decay width for the transition of $p\bar{p}$ atomic states to two-meson final states ϕX can be calculated by

$$\Gamma_{p\bar{p}\to\phi X} = \frac{1}{2E}\int \frac{d^3p_\phi}{2E_\phi}\frac{d^3p_X}{2E_X}\delta^{(3)}(\vec{p}_\phi + \vec{p}_X)\delta(E - E_\phi - E_X) \times |T_{f,i}(\vec{q})|^2, \quad (20)$$

where E is the total energy ($E = 1.876$ GeV) and $E_{\phi,X} = \sqrt{m_{\phi,X}^2 + \vec{p}_{\phi,X}^2}$ is the energy of the outgoing mesons ϕ and X with mass $m_{\phi,X}$ and momentum $\vec{p}_{\phi,X}$. With the obtained transition amplitude given by Eqs. (12) and (19), the partial decay width for the transition from the $p\bar{p}$ atomic state $|i\rangle = |ILSJ\rangle$ can be written as

$$\Gamma_{p\bar{p}\to\phi X} = |AB|^2\lambda_{A_1}^2 f(\phi,X)\langle f|O_{A_1}|i\rangle^2\gamma_i(I). \quad (21)$$

Here, the function $f(\phi,X)$ is the kinematical phase-space factor depending on the relative momentum and the masses of ϕX system, while $\gamma_i(I)$ is the factor depending on the initial-state interaction. Thus, the branching ratio BR of the annihilation reactions at rest $p\bar{p}\to\phi X(X = \pi^0,\eta,\rho^0,\omega)$ can be expressed as

$$\text{BR}_i(\phi,X) = \frac{(2J+1)\Gamma_{p\bar{p}\to\phi X}}{\Gamma_{\text{tot}}(i)}, \quad (22)$$

where $(2J+1)$ are the statistical weights corresponding to the initial values of the total angular momentum J. The fraction $\Gamma_{\text{tot}}(i)$ denotes the total annihilation width of the $p\bar{p}$ atomic state with fixed principal quantum number [26].

The functions $\gamma_i(I)$, depending on the initial-state interaction, are related to the probability of a protonium state to have isospin I and spin J. We adopt the probability $\gamma_i(I)$ and the total decay width $\Gamma_{\text{tot}}(J)$ obtained in an optical potential calculation [24,26]. The model dependence due to the harmonic oscillator approximation may be reduced by applying a simplified phenomenological approach for $N\bar{N}$ annihilation [20,27]. Instead of the obtained kinematical phase-space factor $f(\phi,X)$, we use the phenomenological form,

$$f(\phi,X) = q\exp\{-1.2\ \text{GeV}^{-1}\,(s - s_{\phi X})^{1/2}\}, \quad (23)$$

where $s_{\phi X} = (m_\phi + m_X)^{1/2}$ and $\sqrt{s} = (m_\phi^2 + q^2)^{1/2} + (m_X^2 + q^2)^{1/2}$. The kinematical phase-space factor in Eq. (23) has been fitted to the cross section of various annihilation channels [28]. Other alternative correcting factors can be found in the literature. For instance, one may use the phase-space factor $pF_L^2(q)$, where $F_L(q)$ is the so-called Blatt-Weisskopf damping factor depending on the final state orbital angular momentum L, to account more or less for the final-state interaction in $p\bar{p}$ annihilations into two mesons. The explicit forms of $F_L(q)$ can be found in Table IV in Ref. [2]. For the annihilation reactions in this work, however, $F_L(q)$ simply take the value 1, as the final momentum is much higher than the so-called cutoff momentum, 197 MeV. Both the phase-space factor in Eq. (23) and the Blatt-Weisskopf damping form have merits in the investigation of the low-energy $p\bar{p}$ annihilations, but it is clear that the factor in Eq. (23) is more suitable to the present work.

The obtained theoretical results for branching ratios of Eq. (22) for each $uuds\bar{s}$ configuration of the S to P ($L = 0$, $\ell_f = 1$) and P to S ($L = 1$, $\ell_f = 0$) transitions are compared with the experimental data (BR$^{\text{exp}}$) in Tables III and IV, respectively. To eliminate the factor $|AB|^2\lambda_{A_1}^2$ which is unknown *a priori*, the model predictions of one entry (as indicated by $\star$) have been normalized to the experimental number. Therefore, the obtained branching ratios cannot be used for estimating the pentaquark content (the coefficient B) in the nucleon. For the transition $p\bar{p}\to\phi\eta$, the physical η meson is produced by its nonstrange component η_{ud} with $\eta = \eta_{ud}(\sqrt{1/3}\cos\theta - \sqrt{2/3}\sin\theta)$, with the pseudoscalar mixing angle θ varying from -10.7° to -20°. As shown in Tables III and IV, the model predictions with flavor-spin mixed symmetry $[4]_{\text{FS}}$ are in good agreement with the experimental data. Especially, excellent agreement is found in the configuration with flavor-spin symmetry $[4]_{\text{FS}}[22]_F[22]_s$ which gave branching ratios consistent with the experimental data for both the S to P and P to S transitions.

TABLE III. Branching ratio BR ($\times 10^4$) for the transition $p\bar{p} \to \phi X$ ($X = \pi^0, \eta, \rho^0, \omega$) in $p\bar{p}$ s-wave state annihilations at rest, with the initial state denoted by ${}^{2I+1,2S+1}L_J$. The results indicated by ⋆ have been normalized to the experimental values.

	${}^{11}S_0 \to \omega\phi$	${}^{33}S_1 \to \pi^0\phi$	${}^{31}S_0 \to \rho^0\phi$	${}^{13}S_1 \to \eta\phi$
BR^{exp}	6.3 ± 2.3	5.5 ± 0.7	3.4 ± 1.0	0.9 ± 0.3
[4][22][22]	6.3⋆	5.4	3.8	1.4–1.8
[4][31][31]	6.3⋆	5.4	3.8	1.4–1.8
[31][211][22]	6.3⋆	4.3	3.8	1.9–2.5
[31][211][31]	6.3⋆	3.8	2.7	1.2–1.5
[31][22][31]	6.3⋆	5.9	4.9	1.0–1.4
[31][31][22]	6.3⋆	7.3	3.9	0.90–1.0
[22][211][31]	6.3⋆	181.2	97.5	44.0–57.6
[31][31][31]	6.3⋆	10.0	6.3	2.7–3.6
[22][22][22]	6.3⋆	0.85	3.4	5.3–6.9
[211][211][22]	6.3⋆	0.85	3.5	5.3–6.7
[211][211][31]	6.3⋆	7.7	4.0	3.2–4.2
[22][31][31]	6.3⋆	4.5	2.3	2.2–2.9
[211][22][31]	6.3⋆	181.2	97.5	44.0–57.6
[211][31][22]	6.3⋆	0.85	3.5	5.3–6.9
[211][31][31]	6.3⋆	0.24	0.17	0.090–0.11

IV. SUMMARY

We have estimated the branching ratios of the annihilation reactions at rest $p\bar{p} \to \phi X$ ($X = \pi^0, \eta, \rho^0, \omega$) from atomic $p\bar{p}$ S- and P-wave states in the effective quark line diagrams incorporating the ${}^3P_0$ model. The proton wave functions are assumed to include the intrinsic strangeness in the form of $qqqs\bar{s}$ components. Considered in the work are 15 $qqqs\bar{s}$ configurations, where the subsystem *uuds* is in the P state but the $\bar{s}$ is in the S state relative to the *uuds* subsystem, since these configurations lead to negative strangeness spin σ_s and positive magnetic moment μ_s.

It is shown in Table III that the theoretical results with flavor-spin symmetries $[4]_{FS}[22]_F[22]_s$, $[4]_{FS}[31]_F[31]_s$, $[31]_{FS}[211]_F[31]_s$, $[31]_{FS}[22]_F[31]_s$, and $[31]_{FS}[31]_F[22]_s$ for the pentaquark components are consistent with the experimental data for $p\bar{p}$ annihilation in the S wave. Table IV shows that for $p\bar{p}$ annihilation in the P wave the pentaquark configurations with flavor-spin symmetries $[4]_{FS}[22]_F[22]_s$ and $[31]_{FS}[211]_F[22]_s$ lead to theoretical predictions consistent with the experimental data. Therefore, one may conclude that the best agreement of theoretical results with the experimental data is found in the pentaquark configuration with flavor-spin symmetry $[4]_{FS}[22]_F[22]_s$.

ACKNOWLEDGMENTS

This work was partly supported by the Suranaree University of Technology (SUT) under Grant No. SUT1-105-57-12-27 and by the Thailand Research Fund (TRF) under Grant No. IRG57800010. S.S .acknowledges support from the Faculty of Science, Burapha University. A.K. and Y.Y. acknowledge support from SUT under the SUT-CHE-NRU Project (Grant No. NV. 4/2558).

APPENDIX A: COLOR WAVE FUNCTIONS OF q^4 CLUSTERS

The q^4 color wave functions can be derived by applying the λ-type, ρ-type, and η-type projection operators of the irreducible representation IR[211] of the permutation group S_4 in the Yamanouchi basis onto single-particle color states. For the product state $RRGB$, for example, we have,

$$\begin{aligned} P_{[211]_\lambda}(RRGB) &\Longrightarrow \chi^c_{[211]_\lambda}(R), \\ P_{[211]_\rho}(RGRB) &\Longrightarrow \chi^c_{[211]_\rho}(R), \\ P_{[211]_\eta}(RGBR) &\Longrightarrow \chi^c_{[211]_\eta}(R), \end{aligned} \tag{A1}$$

TABLE IV. Branching ratio BR ($\times 10^4$) for the transition $p\bar{p} \to \phi X$ ($X = \pi^0, \eta, \rho^0, \omega$) in $p\bar{p}$ p-wave state annihilations at rest.

	${}^{33}P_{0,1,2} \to \rho^0\phi$	${}^{31}P_1 \to \pi^0\phi$	${}^{13}P_{0,1,2} \to \omega\phi$	${}^{11}P_1 \to \eta\phi$
BR^{exp}	3.7 ± 0.9	$0 + 0.3$	2.9 ± 1.4	0.4 ± 0.2
[4][22][22]	3.7⋆	0.31	1.6	0.10–0.14
[4][31][31]	3.7⋆	1.1	5.3	0.36–0.47
[31][211][22]	3.7⋆	0.48	1.3	0.17–0.22
[31][211][31]	3.7⋆	1.4	6.1	0.55–0.71
[31][22][31]	3.7⋆	0.65	5.1	0.18–0.23
[31][31][22]	3.7⋆	0.22	2.5	0.067–0.087
[22][211][31]	3.7⋆	0.012	0.23	$(1.2–1.5)\times 10^{-5}$
[31][31][31]	3.7⋆	0.76	2.4	0.26–0.34
[22][22][22]	3.7⋆	0.0029	13	0.0061–0.0080
[211][211][22]	3.7⋆	0.0029	13	0.0061–0.0080
[211][211][31]	3.7⋆	0.0029	3.6	0.23–0.30
[22][31][31]	3.7⋆	5.1×10^{-4}	2.2	0.16–0.20
[211][22][31]	3.7⋆	0.012	0.23	$(1.2–1.5)\times 10^{-5}$
[211][31][22]	3.7⋆	0.0029	13	0.0061–0.0080
[211][31][31]	3.7⋆	7.4×10^{-4}	0.63	0.0062–0.0081

with

$$\chi^c_{[211]_\lambda}(R) = \frac{1}{\sqrt{16}}(2|RRGB\rangle - 2|RRBG\rangle - |GRRB\rangle - |RGRB\rangle - |BRGR\rangle - |RBGR\rangle + |BRRG\rangle + |GRBR\rangle + |RBRG\rangle + |RGBR\rangle),$$

$$\chi^c_{[211]_\rho}(R) = \frac{1}{\sqrt{48}}(3|RGRB\rangle - 3|GRRB\rangle + 3|BRRG\rangle - 3|RBRG\rangle + 2|GBRR\rangle - 2|BGRR\rangle - |BRGR\rangle + |RBGR\rangle + |GRBR\rangle - |RGBR\rangle),$$

$$\chi^c_{[211]_\eta}(R) = \frac{1}{\sqrt{6}}(|BRGR\rangle + |RGBR\rangle + |GBRR\rangle - |RBGR\rangle - |GRBR\rangle - |BGRR\rangle). \quad \text{(A2)}$$

APPENDIX B: WAVE FUNCTIONS OF MESONS, q^3, AND $q^4\bar{q}$ SYSTEMS

The wave functions of the mesons M (ϕ and X), $\bar{p}$ ($\bar{q}^3$), and $q^4\bar{q}$ systems, which are employed in this work, can be expressed in terms of the quark momenta as

$$\begin{aligned}\langle \vec{q}_{i'}\vec{q}_{j'}|M\rangle &\equiv \varphi_M(\vec{q}_{i'},\vec{q}_{j'})\chi_M(q\bar{q}) \\ &= N_M \exp\left\{-\frac{R_M^2}{8}(\vec{q}_{i'}-\vec{q}_{j'})^2\right\}\chi_M(q\bar{q}), \\ \langle \vec{q}_6\vec{q}_7\vec{q}_8|\bar{u}\bar{u}\bar{d}\rangle &\equiv \varphi_{\bar{p}}(\vec{q}_6,\vec{q}_7,\vec{q}_8)\chi_{\bar{p}}(\bar{q}^3) \\ &= N_B \exp\left\{-\frac{R_B^2}{4}\left[(\vec{q}_7-\vec{q}_8)^2 + \frac{(\vec{q}_7+\vec{q}_8-2\vec{q}_6)^2}{3}\right]\right\}\chi_{\bar{p}}(\bar{q}^3),\end{aligned} \quad \text{(B1)}$$

respectively, where $N_M = (R_M^2/\pi)^{3/4}$ and $N_B = (3R_B^2/\pi)^{3/2}$, with $R_{(M,B)}$ being the meson (baryon) radial parameter. Here, $\chi_M(q\bar{q})$ and $\chi_B(\bar{q}^3)$ denote the spin-flavor-color wave function, $[S]\otimes[F]\otimes[C]$. Note that the internal spatial wave functions are approximated as the harmonic oscillator forms.

In case of *uuds* quarks in their ground state with the spatial state symmetry $[4]_O$, the full $5q$ component wave function is given by

$$\langle \vec{q}_1...\vec{q}_5|uuds\bar{s}\rangle = \varphi_{uuds\bar{s}}(\vec{q}_1,\ldots,\vec{q}_5)Y_{1\mu}\left(\frac{\vec{q}_2+\vec{q}_3+\vec{q}_4+\vec{q}_5-4\vec{q}_1}{\sqrt{20}}\right)\psi_{uuds\bar{s}}, \quad \text{(B2)}$$

with

$$\varphi_{uuds\bar{s}}(\vec{q}_1,..,\vec{q}_5) = N_{uuds\bar{s}}\exp\left\{-\frac{R^2_{uuds\bar{s}}}{4}\left[(\vec{q}_2-\vec{q}_3)^2 + \frac{(\vec{q}_2+\vec{q}_3-2\vec{q}_4)^2}{3} + \frac{(\vec{q}_2+\vec{q}_3+\vec{q}_4-3\vec{q}_5)^2}{6} + \frac{(\vec{q}_2+\vec{q}_3+\vec{q}_4+\vec{q}_5-4\vec{q}_1)^2}{10}\right]\right\}, \quad \text{(B3)}$$

where $\psi_{uuds\bar{s}}$ is the spin-flavor-color wave function as defined in Eq. (8).

The $5q$ wave function for the *uuds* subsystem with orbital angular momentum $\ell = 1$ can be constructed systematically in the group theory approach mentioned in Sec. II. For instance, for the simplest case where the spin-flavor part of the q^4 subsystem takes the $[4]_{\rm FS}$ symmetry, the wave function takes the form

$$\langle uuds\bar{s}|\vec{q}_1\cdots\vec{q}_5\rangle = \varphi_{uuds\bar{s}}(\vec{q}_1,\ldots,\vec{q}_5)\psi_{uuds\bar{s}}, \quad \text{(B4)}$$

where $\varphi_{uuds\bar{s}}(\vec{q}_1,\ldots,\vec{q}_5)$ has the same form as that shown in Eq. (B3). Here, $\psi_{uuds\bar{s}}$ representing the spatial-spin-flavor-color wave function of the $5q$ component is derived as

$$\psi_{uuds\bar{s}} = \sum_{J_{4q}}\left[\left|\frac{1}{2},m_{\bar{s}}\right\rangle \otimes \left[\bar{s}\;\chi^{\rm FS}_{[4]_{S_{4q}},m_{4q}}(uuds)\otimes\chi^{\rm OC}_{\ell,\mu}\right]_{J_{4q},m_{4q}}\right]_{\frac{1}{2},m_{5q}}, \quad \text{(B5)}$$

where

$$\chi^{\rm OC}_{1,\mu} = \frac{1}{\sqrt{3}}\left[\chi^C_{[222]_\lambda}Y_{1\mu}\left(\frac{\vec{q}_2-\vec{q}_3}{\sqrt{2}}\right) - \chi^C_{[222]_\rho}Y_{1\mu}\left(\frac{\vec{q}_2+\vec{q}_3-2\vec{q}_4}{\sqrt{6}}\right) + \chi^C_{[222]_\eta}Y_{1\mu}\left(\frac{\vec{q}_2+\vec{q}_3+\vec{q}_4-3\vec{q}_5}{\sqrt{12}}\right)\right] \quad \text{(B6)}$$

for $\ell = 1$, and $J_{4q} = \ell \oplus S_{4q}$ is the total angular momentum for the *uuds* subsystem.

There are three configurations for the q^4 spin-flavor symmetry $[4]_{\rm FS}$, that is, $[22]_F[22]_S$, $[31]_F[31]_S$, and $[4]_F[4]_S$ as shown in Table II, and hence three q^4 spin-flavor wave functions $\chi^{\rm FS}_{[4]}$ as follows:

$$\chi^{\rm FS}_{[4]_{S_{4q}=0}} = \sum_{i,j} a_{ij}\chi^F_{[22]_i}\chi^S_{[22]_j}, \quad \chi^{\rm FS}_{[4]_{S_{4q}=1}} = \sum_{i,j} a_{ij}\chi^F_{[31]_i}\chi^S_{[31]_j},$$
$$\chi^{\rm FS}_{[4]_{S_{4q}=2}} = \sum_{i,j} a_{ij}\chi^F_{[4]_i}\chi^S_{[4]_j}. \quad \text{(B7)}$$

It is an easy task to determine the coefficients by applying the S_4 representations in Yamanouchi basis onto the above equations. The explicit forms of the spin and flavor wave functions can be work out in the approach of projection operators as shown in Sec. II for the color wave functions.

APPENDIX C: THE SPIN-ANGULAR MOMENTUM FUNCTIONS AND THE GEOMETRICAL CONSTANTS

The spin-angular momentum functions $f_{m,n}^{\mathrm{SP(PS)}}(\nu,\mu,\lambda,L,M,l_f,m_f)$ in Eq.(13) are given by

$$\begin{aligned}
f_{1,1}^{\mathrm{SP}} &= f_{1,2}^{\mathrm{SP}} = f_{1,3}^{\mathrm{SP}} = (-1)^{\nu}\delta_{\lambda,-\nu}\delta_{\mu,m_f},\\
f_{2,1}^{\mathrm{SP}} &= f_{2,2}^{\mathrm{SP}} = f_{2,3}^{\mathrm{SP}} = (-1)^{\mu}\delta_{\mu,-\nu}\delta_{\lambda,m_f},\\
f_{3,1}^{\mathrm{SP}} &= f_{3,2}^{\mathrm{SP}} = f_{3,3}^{\mathrm{SP}} = (-1)^{\mu}\delta_{\mu,-\lambda}\delta_{\nu,m_f},\\
f_{1,1}^{\mathrm{PS}} &= f_{1,2}^{\mathrm{PS}} = f_{1,3}^{\mathrm{PS}} = (-1)^{\lambda+\mu}\delta_{\lambda,-\nu}\delta_{\mu,-M},\\
f_{2,1}^{\mathrm{PS}} &= f_{2,2}^{\mathrm{PS}} = f_{2,3}^{\mathrm{PS}} = (-1)^{\lambda+\mu}\delta_{\mu,-\nu}\delta_{\lambda,-M},\\
f_{3,1}^{\mathrm{PS}} &= f_{3,2}^{\mathrm{PS}} = f_{3,3}^{\mathrm{PS}} = (-1)^{\nu+\mu}\delta_{\mu,-\lambda}\delta_{\nu,-M}.
\end{aligned} \tag{C1}$$

The geometrical constants Q_k^2, Q_q^2 and $\Omega_{m,n}^{\mathrm{SP(PS)}}$, in Eq.(13), depending on the meson and baryon size parameters, are given as follows:

$$\begin{aligned}
Q_k^2 &= -\frac{R_M^4}{9\left(3\left(R_B^2+R_{uuds\bar{s}}^2\right)+2R_M^2\right)}+\frac{R_M^2}{18}+\frac{R_{uuds\bar{s}}^2}{15}\\
Q_p^2 &= \frac{12R_B^2\left(R_M^2+6R_{uuds\bar{s}}^2\right)+R_{uuds\bar{s}}^2\left(28R_M^2+15R^2+25R_{uuds\bar{s}}^2\right)}{32\left(3R_B^2+2R_M^2+3R_{uuds\bar{s}}^2\right)},\\
\Omega_{1,1}^{\mathrm{SP}} &= -\frac{\sqrt{3}(\beta_2+4\beta_3+4\beta_4+3)(2Q_3-Q_4)(2Q_3+Q_4)}{8Q_2^3Q_3^5Q_4^5},\\
\Omega_{2,1}^{\mathrm{SP}} &= -\frac{\sqrt{3}(\beta_3+\beta_4+1)(2Q_3-Q_4)(2Q_3+Q_4)}{2Q_2^3Q_3^5Q_4^5},\\
\Omega_{3,1}^{\mathrm{SP}} &= -\frac{\sqrt{3}\beta_4\left(4Q_3^2+Q_4^2\right)}{2Q_2^3Q_3^5Q_4^5},\\
\Omega_{1,2}^{\mathrm{SP}} &= -\frac{\sqrt{\frac{3}{2}}(\beta_2+\beta_3-2\beta_4)\left(4Q_3^2-Q_4^2\right)}{4Q_2^3Q_3^5Q_4^5},\\
\Omega_{2,2}^{\mathrm{SP}} &= \frac{\sqrt{\frac{3}{2}}(\beta_3+\beta_4+1)\left(2Q_3^2+Q_4^2\right)}{Q_2^3Q_3^5Q_4^5},\\
\Omega_{3,2}^{\mathrm{SP}} &= \frac{\sqrt{\frac{3}{2}}\beta_4\left(2Q_3^2-Q_4^2\right)}{Q_2^3Q_3^5Q_4^5},\\
\Omega_{1,3}^{\mathrm{SP}} &= -\frac{3(\beta_2-\beta_3)\left(4Q_3^2-Q_4^2\right)}{4\sqrt{2}Q_2^3Q_3^5Q_4^5},\\
\Omega_{2,3}^{\mathrm{SP}} &= -\frac{3(\beta_3+\beta_4+1)}{2\sqrt{2}Q_2^3Q_3^5Q_4^3},\\
\Omega_{3,3}^{\mathrm{SP}} &= \frac{3\beta_4}{2\sqrt{2}Q_2^3Q_3^5Q_4^3},\\
\Omega_{1,1}^{\mathrm{PS}} &= -\frac{\sqrt{3}(\alpha_2+4\alpha_3+4\alpha_4-3)\left(4Q_3^2-Q_4^2\right)}{8Q_2^3Q_3^5Q_4^5},\\
\Omega_{2,1}^{\mathrm{PS}} &= -\frac{\sqrt{3}(\alpha_3+\alpha_4-1)\left(4Q_3^2-Q_4^2\right)}{2Q_2^3Q_3^5Q_4^5},\\
\Omega_{3,1}^{\mathrm{PS}} &= -\frac{\sqrt{3}\alpha_4\left(4Q_3^2+Q_4^2\right)}{2Q_2^3Q_3^5Q_4^5},\\
\Omega_{1,2}^{\mathrm{PS}} &= -\frac{\sqrt{\frac{3}{2}}(\alpha_2+\alpha_3-2\alpha_4)\left(4Q_3^2-Q_4^2\right)}{4Q_2^3Q_3^5Q_4^5},\\
\Omega_{2,2}^{\mathrm{PS}} &= \frac{\sqrt{\frac{3}{2}}(\alpha_3+\alpha_4-1)\left(2Q_3^2+Q_4^2\right)}{Q_2^3Q_3^5Q_4^5},\\
\Omega_{3,2}^{\mathrm{PS}} &= \frac{\sqrt{\frac{3}{2}}\alpha_4\left(2Q_3^2-Q_4^2\right)}{Q_2^3Q_3^5Q_4^5},\\
\Omega_{1,3}^{\mathrm{PS}} &= -\frac{3(\alpha_2-\alpha_3)\left(4Q_3^2-Q_4^2\right)}{4\sqrt{2}Q_2^3Q_3^5Q_4^5},\\
\Omega_{2,3}^{\mathrm{PS}} &= -\frac{3(\alpha_3+\alpha_4-1)}{2\sqrt{2}Q_2^3Q_3^5Q_4^3},\\
\Omega_{3,3}^{\mathrm{PS}} &= \frac{3\alpha_4}{2\sqrt{2}Q_2^3Q_3^5Q_4^3},
\end{aligned} \tag{C2}$$

where

$$\begin{aligned}
Q_2^2 &= \frac{R_M^2}{2}+R_{uuds\bar{s}}^2,\\
Q_3^2 &= \frac{1}{4}\left[2R_M^2+3\left(R_B^2+R_{uuds\bar{s}}^2\right)\right],\\
Q_4^2 &= R_B^2+R_{uuds\bar{s}}^2,\\
\alpha_2 &= 0,\\
\alpha_3 &= -\frac{-R_B^2-R_{uuds\bar{s}}^2}{2R_M^2+3R_B^2+3R_{uuds\bar{s}}^2},\\
\alpha_4 &= -\frac{-R_M^2-R_B^2-R_{uuds\bar{s}}^2}{2R_M^2+3R_B^2+3R_{uuds\bar{s}}^2},\\
\beta_2 &= 1/2,\\
\beta_3 &= -\frac{R_M^2+3R_B^2+R_{uuds\bar{s}}^2}{2R_M^2+3R_B^2+3R_{uuds\bar{s}}^2},\\
\beta_4 &= -\frac{R_M^2+2R_{uuds\bar{s}}^2}{2\left(2R_M^2+3R_B^2+3R_{uuds\bar{s}}^2\right)}.
\end{aligned} \tag{C3}$$

[1] C. Amsler, in *Intersections Between Particle and Nuclear Physics*, May 1991, Tucson, AZ, edited by W. T. H. Van Oers, AIP Conf. Proc. No. 243 (AIP, New York, 1992), p. 263.

[2] C. Amsler, Rev. Mod. Phys. **70**, 1293 (1998).

[3] D. S. Armstrong and R. D. McKeown, Annu. Rev. Nucl. Part. Sci. **62**, 337 (2012).

[4] M. Diehl, T. Feldmann, and P. Kroll, Phys. Rev. D **77**, 033006 (2008).

[5] D. H. Beck and R. D. McKeown, Annu. Rev. Nucl. Part. Sci. **51**, 189 (2001).
[6] J. Green, S. Meinel, M. Engelhardt, S. Krieg, J. Laeuchli, J. Negele, K. Orginos, A. Pochinsky, and S. Syritsyn, Phys. Rev. D **92**, 031501(R) (2015).
[7] C. S. An, D. O. Riska, and B. S. Zou, Phys. Rev. C **73**, 035207 (2006).
[8] B. W. Filippone and X. D. Ji, Adv. Nucl. Phys. **26**, 1 (2001).
[9] D. O. Riska and B. S. Zou, Phys. Lett. B **636**, 265 (2006).
[10] A. Kiswandhi, H. C. Lee, and S. N. Yang, Phys. Lett. B **704**, 373 (2011).
[11] C. S. An and B. Saghai, Phys. Rev. C **88**, 025206 (2013).
[12] C. S. An and B. S. Zou, Eur. Phys. J. A **39**, 195 (2009).
[13] B. Julia-Diaz and D. O. Riska, Nucl. Phys. A **780**, 175 (2006).
[14] Q. B. Li and D. O. Riska, Phys. Rev. C **74**, 015202 (2006).
[15] R. Aaij *et al.* (LHCb Collaboration), Phys. Rev. Lett. **115**, 072001 (2015).
[16] S. Srisuphaphon, Y. Yan, T. Gutsche, and V. E. Lyubovitskij, Phys. Rev. D **84**, 074035 (2011).
[17] J. R. Ellis, M. Karliner, D. E. Kharzeev, and M. G. Sapozhnikov, Phys. Lett. B **353**, 319 (1995).
[18] R. D. Young, in *Achievements and New Directions in Subatomic Physics*, February 2010, Adelaide, edited by W. Melnitchouk, AIP Conf. Proc. 1261 (AIP, New York, 2010), p. 153.
[19] Y. Yan and S. Srisuphaphon, Prog. Part. Nucl. Phys. **67**, 496 (2012).
[20] T. Gutsche, A. Faessler, G. D. Yen, and S. N. Yang, Nucl. Phys. Proc. Suppl. **56**, 311 (1997).
[21] A. Le Yaouanc, L. Oliver, O. Pene, and J. C. Raynal, *Hadron Transitions in the Quark Model* (Gordon and Breach, New York, 1988).
[22] C. B. Dover, T. Gutsche, M. Maruyama, and A. Faessler, Prog. Part. Nucl. Phys. **29**, 87 (1992).
[23] A. Kercek, T. Gutsche, and A. Faessler, J. Phys. G **25**, 2271 (1999).
[24] J. Carbonell, G. Ihle, and J. M. Richard, Z. Phys. A **334**, 329 (1989).
[25] X. W. Kang, J. Haidenbauer, and U. G. Meiner, J. High Energy Phys. 02 (2014) 113.
[26] C. B. Dover, J. M. Richard, and J. Carbonell, Phys. Rev. C **44**, 1281 (1991).
[27] T. Gutsche, R. Vinh Mau, M. Strohmeier-Prešiček, and A. Faessler, Phys. Rev. C **59**, 630 (1999).
[28] J. Vandermeulen, Z. Phys. C **37**, 563 (1988).